CFD Analysis of a Circulation Control Airfoil Using Fluent

Gregory McGowan* and Ashok Gopalarathnam†
North Carolina State University, Raleigh, NC 27695-7910

Abstract

In an effort to validate computational fluid dynamics procedures for calculating flows around circulation control airfoils, the commercial flow solver FLUENT was utilized to study the flow around a general aviation circulation control airfoil. The results were compared to experimental and computational fluid dynamics results conducted at the NASA Langley Research Center. The current effort was conducted in three stages: (i) a comparison of the results for free-air conditions to those from experiments, (ii) a study of wind-tunnel wall effects, and (iii) a study of the stagnation-point behavior. In general the trends in the results from the current work agree well with those from experiment, some differences in magnitude are present between computations and experiment. For the cases examined, FLUENT computations showed no noticeable effect on the results due to the presence of wind-tunnel walls. The study also shows that the leading-edge stagnation point moves in a systematic manner with changes to the jet blowing coefficient and angle of attack, indicating that this location can be sensed for use in closed-loop control of such airfoil flows.

Nomenclature

A	area
b	wing span
c	chord
C_d	drag coefficient
C_l	lift coefficient
C_m	pitching moment coefficient about quarter chord
C_μ	momentum coefficient
h	slot height
$\dot{m}$	mass flow rate
M	Mach number
P	pressure
q	dynamic pressure

*Graduate Research Assistant, Department of Mechanical and Aerospace Engineering, Box 7910. e-mail: gzmcgowa@ncsu.edu.

†Assistant Professor, Department of Mechanical and Aerospace Engineering, Box 7910, (919) 515-5669. e-mail: ashok_g@ncsu.edu.

R gas constant for air
r radius of coanda surface
Re Reynolds number
T temperature
U velocity magnitude
w slot width
α angle of attack
γ ratio of specific heats
μ viscosity
ρ density

Subscripts

$duct$ stagnation conditions inside plenum
fc conditions at flow-control boundary
∞ freestream conditions
J slot-exit conditions

1 Introduction

Recent research in the Applied Aerodynamics Group at NCSU has led to the development of an automated cruise-flap system.[1,2] The cruise flap, introduced by Pfenninger,[3,4] is a small trailing-edge flap which can be used to increase the size of the low-drag range of natural-laminar-flow (NLF) airfoils. The automation is achieved by indirectly sensing the leading-edge stagnation-point location using surface pressure measurements and deflecting the flap so that the stagnation-point location is maintained at the optimum location near the leading-edge of the airfoil. Maintaining the stagnation point at the optimum location results in favorable pressure gradients on both the upper and lower surfaces of the airfoil. With such a cruise-flap system, the airfoil is automatically adapted for a wide speed range. This automated cruise-flap system was successfully tested in the subsonic wind tunnel at NCSU.[2]

While the use of a cruise flap on an NLF airfoil results in low drag over a large range of speeds, there is a need for a revolutionary approach that integrates the achievement of significantly lower drag over a large range of operating speeds with the capability for generating very high lift at takeoff and landing conditions. Toward this objective, it is of interest to study an approach that integrates aerodynamic adaptation with the well-established high-lift capability of circulation control (CC) aerodynamics. This aerodynamic adaptation carries with it the possibility for significant skin-friction drag reductions through extensive laminar flow in addition to the high-lift benefits of CC aerodynamics. Figure 1 illustrates the overall concept. In a manner similar to a cruise flap, it is believed that by utilizing this stagnation-point sensing scheme, an adaptive CC airfoil can achieve extensive laminar flow over a large lift-coefficient range.

As a first step toward the long-term goal of studying an adaptive CC airfoil, the current effort was undertaken for establishing and validating computational fluid dynamics (CFD) analysis procedures for blown-trailing-edge airfoils. The CFD package used for this work was the FLUENT flow solver. The results are compared to CFD and experimental data obtained from a recent study by Jones et al.[5] of a General Aviation CC (GACC) airfoil conducted at the NASA Langley Research Center. Since previous CFD studies on this airfoil did not include tunnel walls, the current CFD

study also includes an investigation of the effect of tunnel walls on the solution. In order to provide a foundation for the adaptive CC airfoil concept, the effects of CC on the leading-edge stagnation-point location was also examined in the current work.

2 Approach

2.1 CFD study

The commercial flow-solver code FLUENT version 6.1 was used in the current research. Grid generation was performed using GAMBIT, which is the preprocessor packaged with the FLUENT code. These codes were used to study two separate cases. The first case involves the examination of the GACC airfoil in free air with the objective of comparing the FLUENT results to CFD and wind-tunnel results presented in Ref. 5. The second case involves simulations of the GACC airfoil in the Basic Aerodynamic Research Tunnel (BART) to examine the influence of tunnel walls on this particular airfoil. Results from FLUENT were obtained for a matrix of 15 data points for both the cases.

2.1.1 Geometry and grid details

The geometry chosen for the current research was the General Aviation Circulation Control (GACC) airfoil, designed by Jones.[5] The GACC airfoil was derived from a 17% GAW(1) airfoil by modifying the trailing edge to incorporate a 2% r/c coanda surface and is shown in Fig. 2.

For the first study, a circular computational domain (Fig. 3) was generated that extends to approximately 20 chord lengths in all directions and is comprised of 132,762 cells. For the study of wall effects, a second grid was generated to include the wind-tunnel geometry and is shown in Fig. 4. The experiments were conducted by Jones et al.[5] in the BART wind-tunnel which is located at the NASA Langley Research Center in Hampton, Va. The BART tunnel has a physical test-section size of 28"$\times$40"$\times$120". The GACC model chord length was 9.4" with angle of attack changes made about the half-chord location. The details of the experimental setup are given in Ref. 6. For the computation with walls, a separate grid was generated for each angle of attack, each of which is comprised of 123,602 cells and extends to 20 chord lengths upstream and downstream of the airfoil.

The grids for all of the analyses are hybrid unstructured grids. The domains consist of an unstructured grid far from the airfoil in order to reduce the number of cells and structured grid near the airfoil in order to maintain good resolution through the boundary and shear layers.

2.1.2 Solver settings

For the current study, the steady, coupled, and implicit solver settings with node-based discretization scheme were selected. The coupled solver was chosen for two reasons. First compressibility effects need to be modeled, as the Mach number at the slot exit can often approach the sonic condition as the blowing rate is increased. Secondly, the FUN2D code has a compressible solver and because the results from the current study were compared with FUN2D results, a compressible solver was also used for the

FLUENT analysis. There was an attempt to run these problems with the segregated (decoupled) solver using very low relaxation factors, however it was found that for the cases with larger blowing rates the solution began to exhibit an unsteady effect after a few thousand iterations. In order to compare with the FUN2D[5] results, the one-equation Spalart-Allmaras turbulence model was chosen.

2.1.3 Boundary conditions

FLUENT does not allow the user to input freestream Mach number and Reynolds number directly. Instead, the freestream velocity and operating pressure were calculated using Eqs. 1–3 and provided as inputs for the analyses. The Mach and Reynolds numbers were set to 0.1 and 533,000, respectively, to match those used in Ref. 5

$$U_\infty = M_\infty \sqrt{\gamma R T_\infty} \tag{1}$$

$$\rho_\infty = \frac{Re \mu_\infty}{U_\infty c} \tag{2}$$

$$P_\infty = \rho_\infty R T_\infty \tag{3}$$

An approximate method was developed to estimate the required velocity at the flow control boundary (U_{fc}) to achieve a desired C_μ, $C_{\mu_{desired}}$. This method assumes incompressible flow throughout the duct, and was derived by solving the continuity equation. The equation for U_{fc} from this approximate method is given in Eq. 4.

$$U_{fc} = U_\infty \sqrt{\frac{C_\mu A_J c b}{2 A_{fc}^2}} \tag{4}$$

Once FLUENT converged, an integration was performed across the slot exit as shown in Eq. 5 to obtain the actual C_μ of the jet at the slot. This C_μ, however, is different from $C_{\mu_{desired}}$ because the U_{fc} for the latter is set using an approximate method.

$$C_{\mu_{integrated}} = \frac{\int_{slot} \rho V^2 \, dy}{\frac{1}{2} \rho_\infty V_\infty^2 c b} \tag{5}$$

Furthermore, in order to be consistent with the methods used for calculating C_μ in Ref. 5, all of the C_μ values presented in this paper were calculated using isentropic flow relations.[5] The equations for this procedure are given in Eqs. 6–8. In order to determine how close the isentropic C_μ is to the integrated C_μ, the two values are compared in Fig. 5 for several cases. The C_μ values indicated along the x-axis are values calculated using the isentropic relations. Values for C_μ on the y-axis were computed by integrating the flow across the slot exit. The solid line in Fig. 5 indicates where the data points would lie if the two methods generated the same values for C_μ. The symbols are representative of the actual values calculated using FLUENT and isentropic relations. Although the differences are very small, care must be taken to ensure consistency in the CFD solutions and experiments.

$$\dot{m} = \rho_J U_J A_J \tag{6}$$

$$U_J = \sqrt{\frac{2\gamma RT_{duct}}{\gamma - 1}\left(1 - \left(\frac{P_\infty}{P_{duct}}\right)^{\frac{\gamma-1}{\gamma}}\right)} \tag{7}$$

$$C_\mu = \frac{\dot{m}U_J}{q_\infty cb} = 2\left(\frac{hw}{cb}\right)\left(\frac{\rho_J}{\rho_\infty}\right)\left(\frac{U_J}{U_\infty}\right)^2 \tag{8}$$

3 Results

The results from FLUENT predictions for the GACC airfoil are presented in three parts. In the first part, the prediction for the GACC airfoil in free-air conditions are compared with the results presented in Ref. 5. In the second part, the predicted results for the GACC airfoil with tunnel walls are presented and compared with the free-air results. In the third part, the effect of α and C_μ on the leading-edge stagnation-point location are presented and discussed.

3.1 Results for free-air conditions

In this part of the study, FLUENT results for free-air conditions are compared with CFD and experimental results from Ref. 5. The comparison is illustrated using C_l-α curves in Fig. 6. The results from FLUENT analyses consist of a matrix of 15 data points for α =−5, 0, and 5 deg and C_μ = 0, 0.008, 0.024, 0.047, and 0.078 and are presented in Fig. 6 using red dashed lines and square markers. The wind-tunnel results from Ref. 5 are presented as blue markers with best-fit lines in Fig. 6 for several angles of attack and for C_μ = 0, 0.007, 0.015, 0.025, 0.041, and 0.060. The values of C_μ for the FLUENT results differ from those for the results of Ref. 5 because of the difference between the actual C_μ and the desired C_μ when using the approximate method in Eq. 4 for estimating the U_{fc} using incompressible-flow equations.

Although the values of C_μ for the FLUENT results do not match those for the results of Ref. 5, it is clear that the trends and most of the predictions for the C_l are close to those from Ref. 5. In particular, the FLUENT predictions for C_μ = 0, 0.008, and 0.047 agree quite well with the results for similar values of C_μ from Ref. 5. Two discrepancies between the FLUENT predictions and those from Ref. 5 are apparent: (i) for the C_μ = 0.024 and (ii) for C_μ = 0.078. The reason for the first discrepancy in the results is attributed to the incorrect prediction of the jet-separation location on the Coanda surface for C_μ = 0.024. The apparent discrepancy in the results for C_μ = 0.078 is attributed to nonlinear effects at the high blowing rates and the fact that the highest blowing rate in the results of Ref. 5 is for C_μ = 0.060.

The flow-field data for the FLUENT results are presented in two separate parts. In the first part, the effects of increasing C_μ for a constant angle of attack is presented. The second part examines the effect of angle-of-attack changes and their influence on the CC airfoil for a constant C_μ. The flow-field data is presented as pressure contours and streamline plots; these aid in the understanding of the effects of CC on the flow over the airfoil.

The first part of the flow-field data is shown in Figs. 7(a)–(c). It can be seen that as the blowing rate is increased the streamlines become more curved — an indication of increased circulation. The second part of the flow-field data is shown in Figs. 8(a)–(c) and Figs. 9(a)–(c) to illustrate the effects of changing the angle of attack while

holding blowing rates constant. The results are presented for two blowing rates: the mild blowing case $C_\mu = 0.047$ and the highest blowing rate $C_\mu = 0.078$. The results show that changes to C_μ have a significant effect on the jet-separation location and the resulting C_l. In comparison, changes to α have a much smaller effect on the jet-separation location.

3.2 Wind-tunnel wall effects

In this sub-section, the FLUENT results for the GACC airfoil with the effect of wind-tunnel walls are presented. Figures 10–12 show the influence of the wall on the CFD solution. These figures present the predicted C_l as a function of C_μ for $\alpha = 0, 5$, and -5 deg respectively. Figure 10 also includes a comparison to results for the FUN2D study[5] for $\alpha = 0$ deg, the only angle of attack for which the FUN2D results were presented in Ref. 5. Figures 10–12 indicate that the presence of walls has very little influence on the CFD solution. The solution, including tunnel walls, consistently show that for low blowing coefficients, the C_l values are predicted to be lower than those without walls. However, at the largest blowing coefficients, the trend reverses and C_l values with walls are predicted to be higher than those without walls.

3.3 Stagnation-point location

The motivation for examining the stagnation-point behavior is that the stagnation-point location was used successfully in earlier research[1,2] for closed-loop control of a trailing-edge flap. It was, therefore, desirable to examine the CFD solutions for the CC airfoils to see if there was any evidence that would suggest that a similar approach could be extended for use with CC airfoils.

Stagnation-point location, measured as an arc length from the jet exit around the upper surface of the airfoil, as a function of C_l is presented in Fig. 13. Each line in Fig. 13 represents a different blowing rate and for each blowing coefficient there are three points that correspond to three different angles of attack($-5, 0$, and 5 deg). From Fig. 13 it can be seen that the stagnation point moves in a predictable manner, both with angle of attack and with changing blowing rate. This behavior provides an indication that the stagnation-point location can be used as a means to develop closed-loop control of the jet C_μ on CC airfoils.

4 Conclusions

The results from a two-part CFD study using the FLUENT flow solver have been presented. Results of the first study show that while the FLUENT predictions do not match the CFD and experimental results of Ref. 5 exactly, the overall trends are followed very closely. Throughout the range of blowing coefficients, FLUENT consistently predicted a slightly lower overall lift coefficient.

In addition, a study was performed on the influence of wind tunnel walls on the CFD solution. For low blowing coefficients, it was found that the lift is predicted to be lower for the cases with walls. The trends are reversed for the higher blowing coefficients, for which the cases with walls yield a higher predicted lift. Although the

solutions are different, the differences are small, and could as well be attributed to differences in the grids rather than the actual presence of walls.

The influence of circulation control on the leading-edge stagnation point location was examined. It was shown that changes in blowing rate and angle of attack result in systematic changes to the stagnation-point location. This observation indicates that it is possible to use a closed-loop control system by sensing the stagnation-point location.

5 Acknowledgments

The authors would like to acknowledge the funding for this research through a grant from the NASA Langley Research Center and the National Institute of Aerospace. The technical monitor, Dr. Greg Jones of NASA Langley, is thanked for many valuable discussions and for the geometry of the GACC airfoil and the wind-tunnel test results. In addition Dr. Greg Stuckert from FLUENT Inc. and Dr. Hassan Hassan of NCSU are thanked for their advice regarding the CFD simulations.

References

[1] McAvoy, C. W. and Gopalarathnam, A., "Automated Cruise Flap for Airfoil Drag Reduction over a Large Lift Range," *Journal of Aircraft*, Vol. 39, No. 6, 2002, pp. 981–988.

[2] McAvoy, C. W. and Gopalarathnam, A., "Automated Trailing-Edge Flap for Airfoil Drag Reduction Over a Large Lift-Coefficient Range," AIAA Paper 2002–2927, June 2002.

[3] Pfenninger, W., "Investigation on Reductions of Friction on Wings, in Particular by Means of Boundary Layer Suction," NACA TM 1181, August 1947.

[4] Pfenninger, W., "Experiments on a Laminar Suction Airfoil of 17 Per Cent Thickness," *Journal of the Aeronautical Sciences*, April 1949, pp. 227–236.

[5] Jones, G. S., Viken, S. A., Washburn, A. E., Jenkins, L. N., and Cagle, C. M., "An Active Flow Circulation Controlled Flap Concept for General Aviation Aircraft Applications," AIAA Paper 2002–3157, 2002.

[6] Cagle, C. M. and Jones, G. S., "A Wind Tunnel Model to Explore Unsteady Circulation Control for General Aviation Applications," AIAA Paper 2002–3240, 2002.

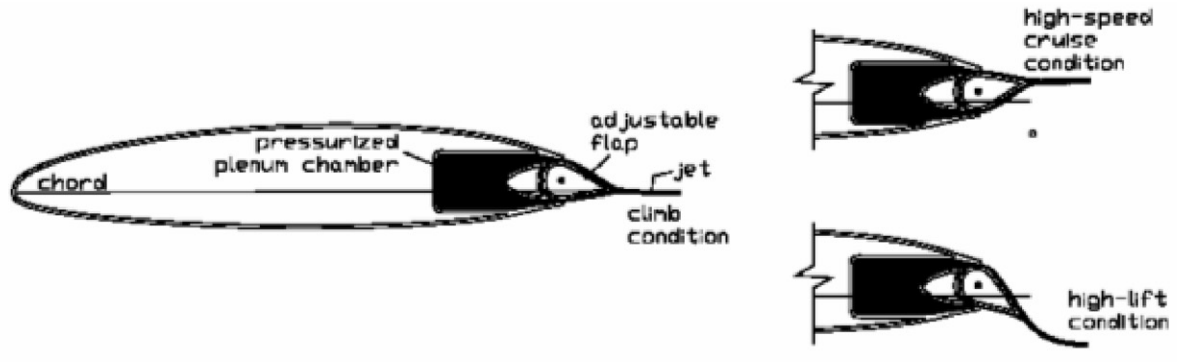

Figure 1: Illustration of the NCSU concept of an adaptive circulation control airfoil.

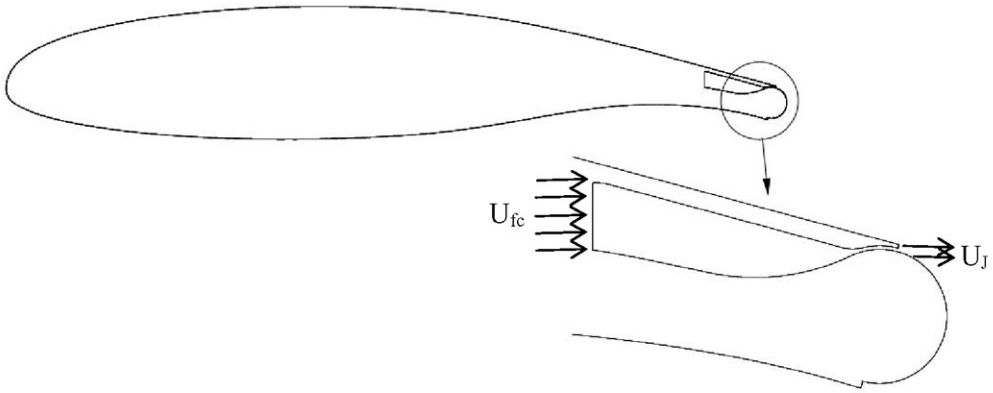

Figure 2: General Aviation Circulation Control (GACC) airfoil geometry used in the current research.

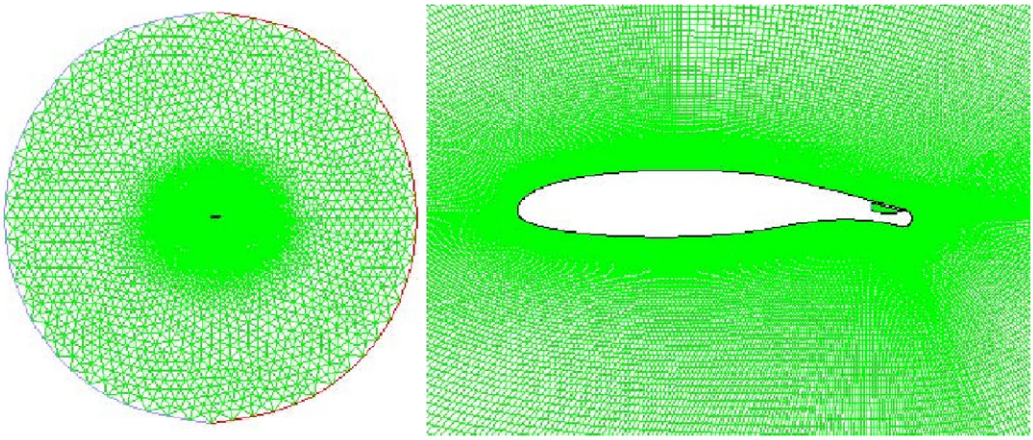

Figure 3: Grid generated for FLUENT comparison to FUN2D.

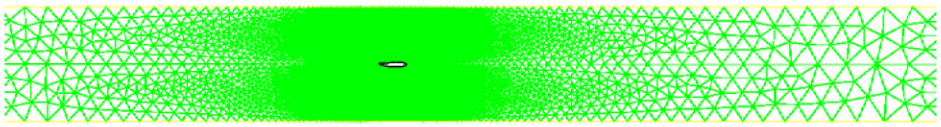

Figure 4: Grid generated for FLUENT study of wall effects.

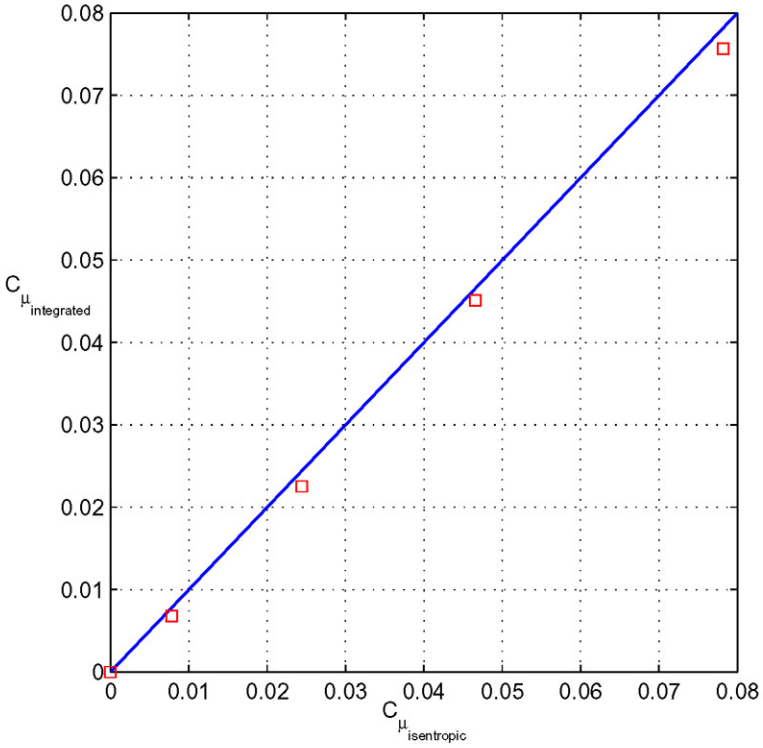

Figure 5: Comparison of $C_{\mu_{integrated}}$ with $C_{\mu_{isentropic}}$ for $\alpha = 0$; the straight line is included to indicate deviation from a perfect correlation.

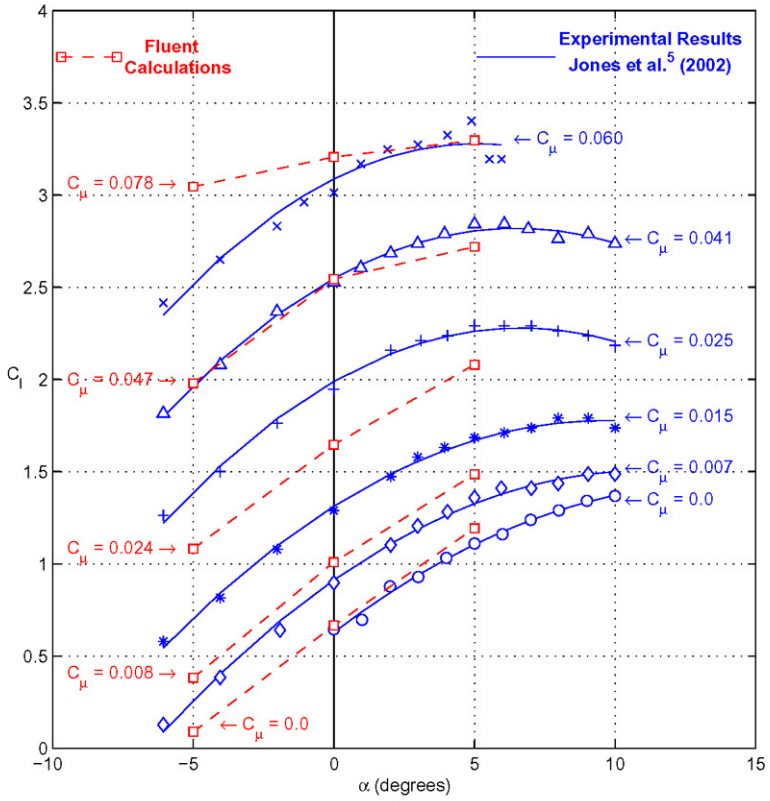

Figure 6: Comparison of Langley experimental and FUN2D analysis with the NCSU FLUENT analysis.

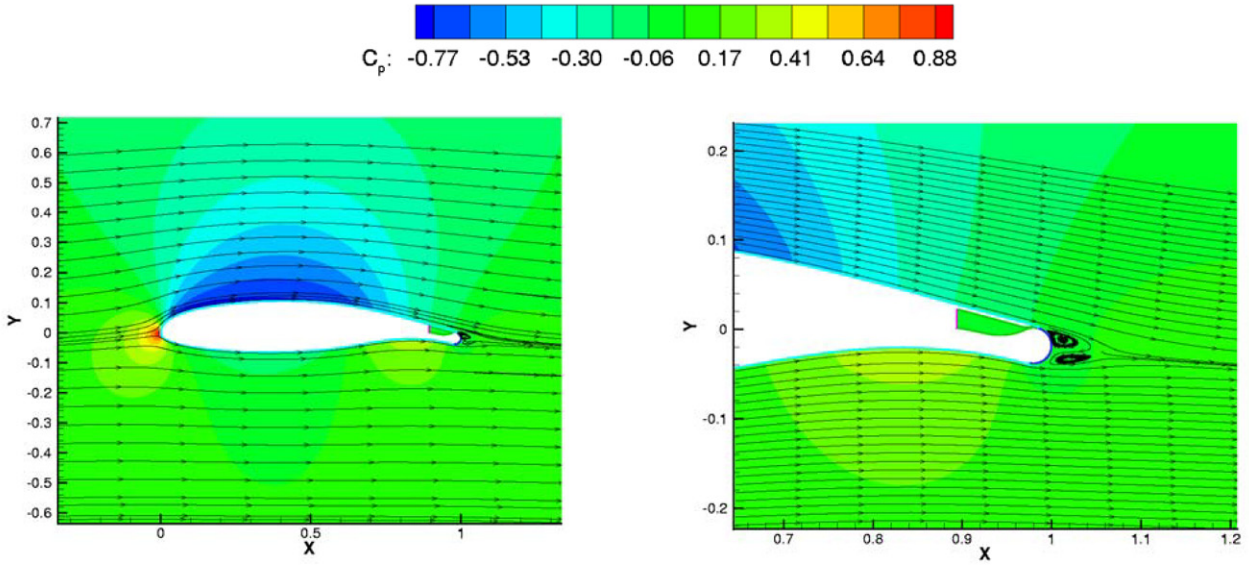

(a) $C_\mu = 0.000$

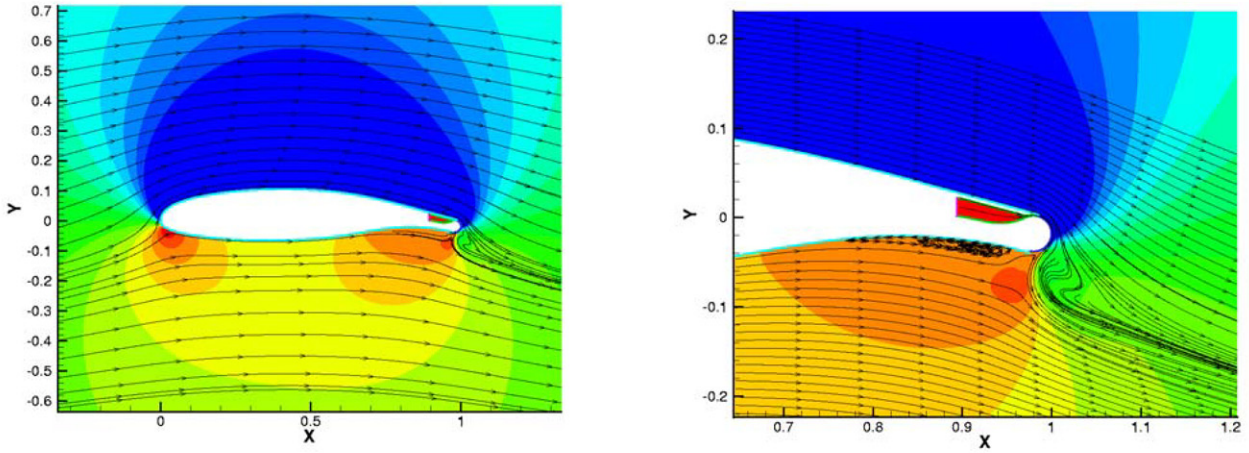

(b) $C_\mu = 0.047$

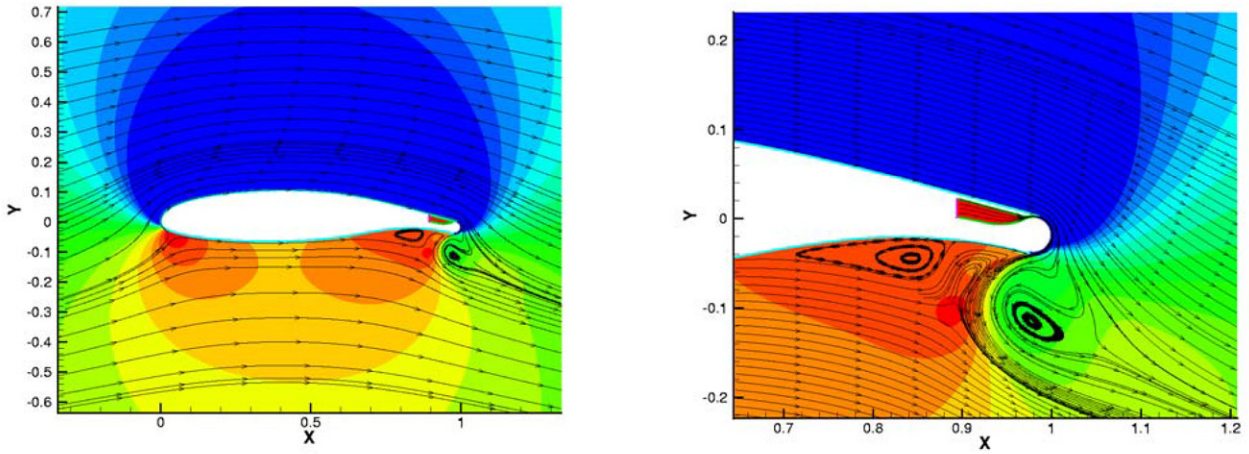

(c) $C_\mu = 0.078$

Figure 7: CC effects on the flow field at $\alpha = 0$ for various values of C_μ.

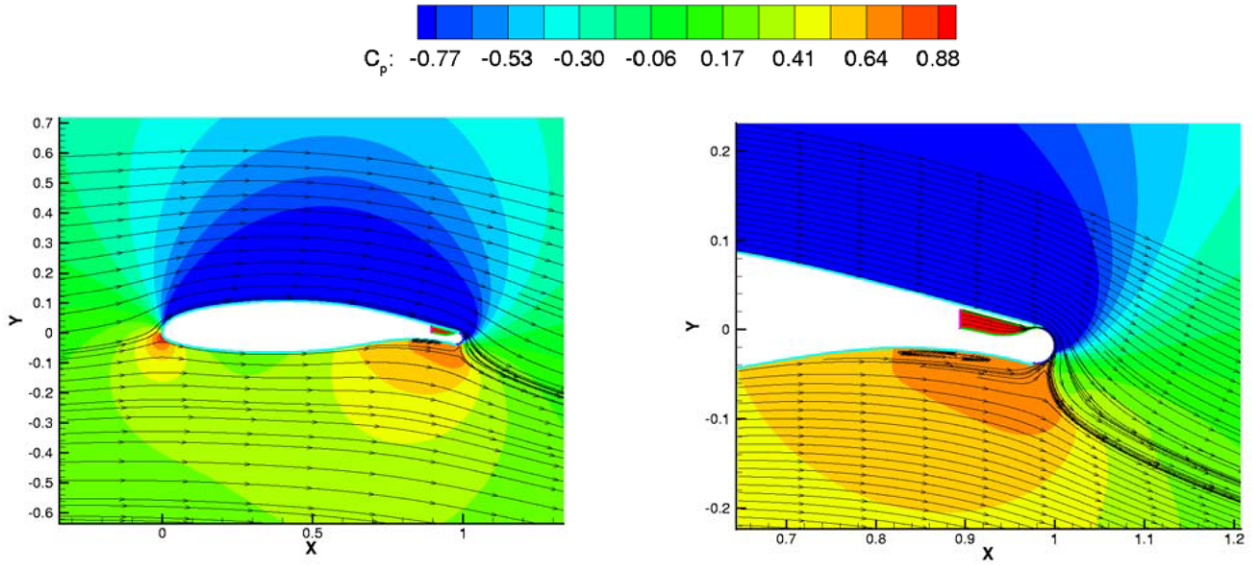

(a) $\alpha = -5$ deg

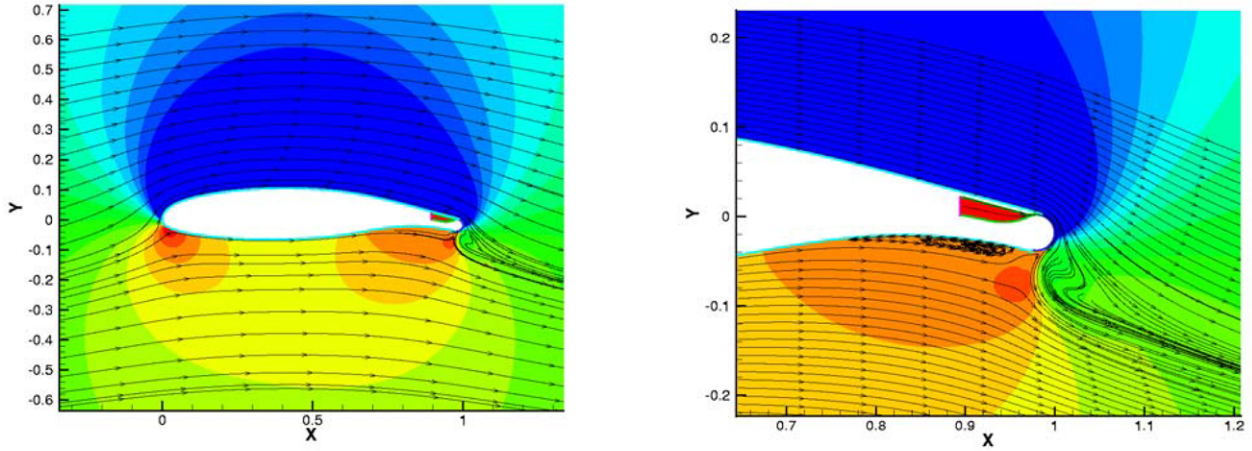

(b) $\alpha = 0$ deg

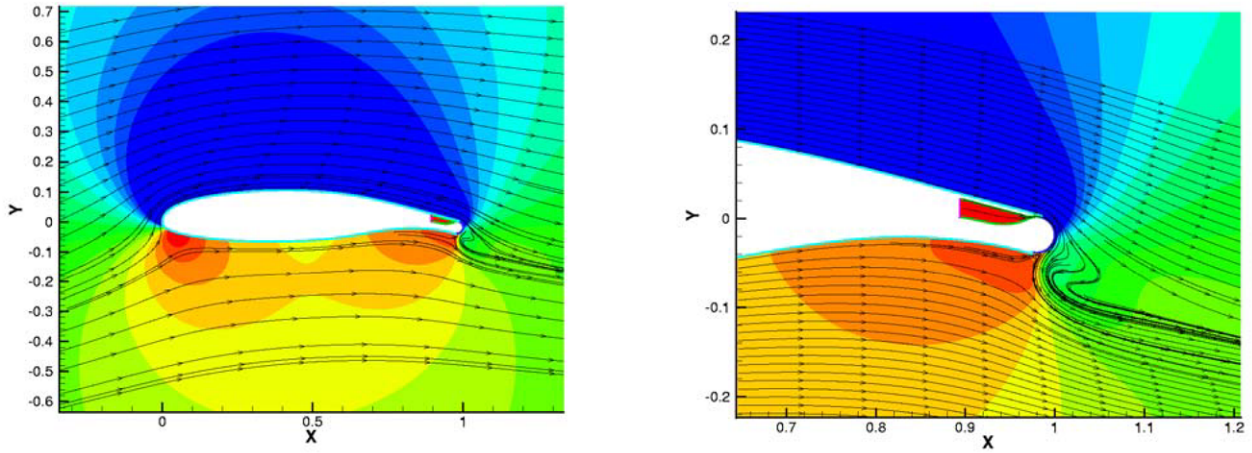

(c) $\alpha = 5$ deg

Figure 8: CC effects on flow field at $C_\mu = 0.047$ for various values of α.

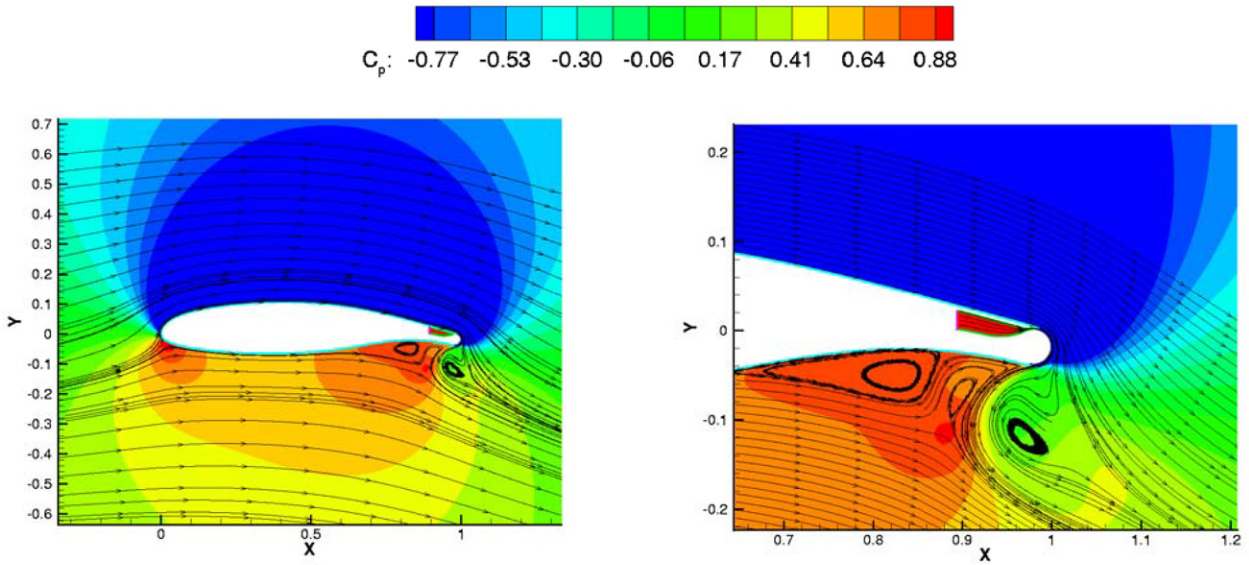

(a) $\alpha = -5$ deg

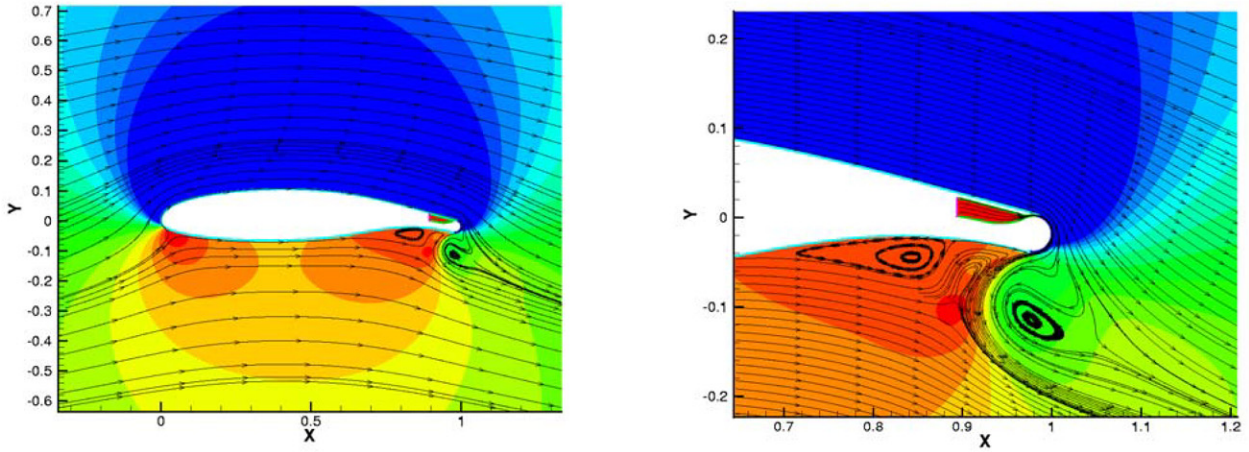

(b) $\alpha = 0$ deg

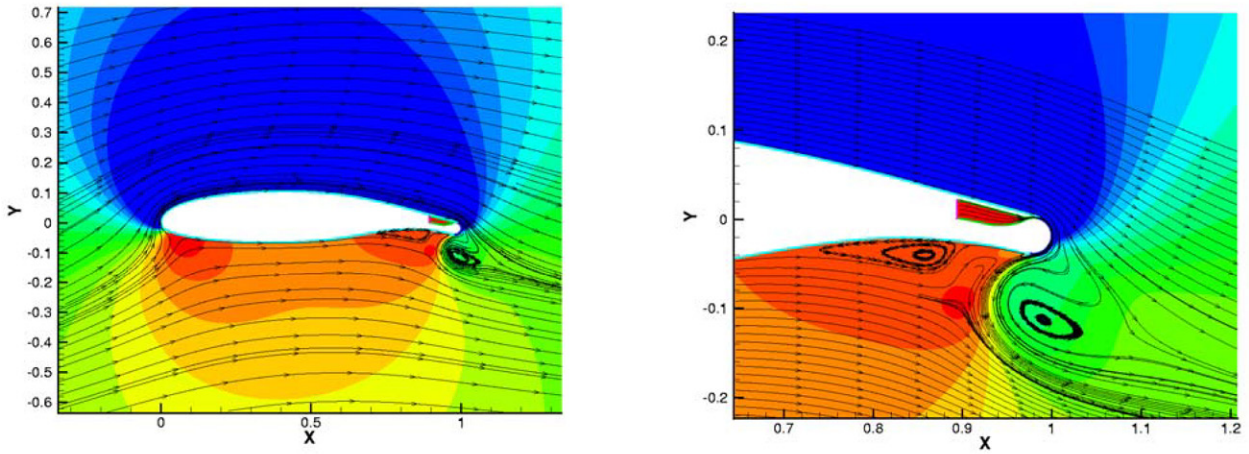

(c) $\alpha = 5$ deg

Figure 9: CC effects on flow field at $C_\mu = 0.078$ for various values of α.

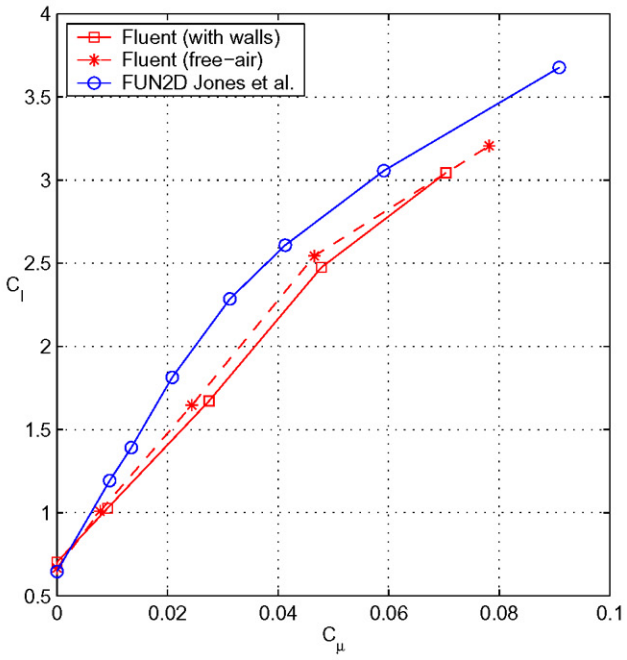

Figure 10: FLUENT prediction of wind-tunnel wall effects for varying values of C_μ at $\alpha = 0$ deg.

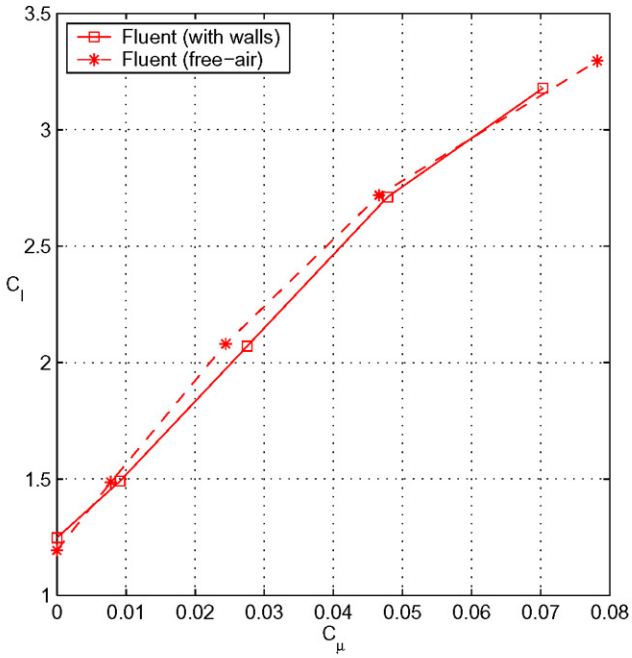

Figure 11: FLUENT prediction of wind-tunnel wall effects for varying values of C_μ at $\alpha = 5$ deg.

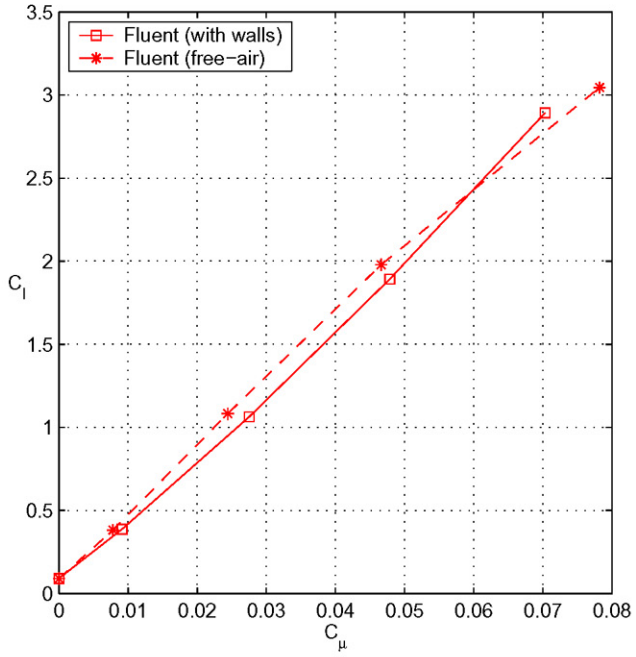

Figure 12: FLUENT prediction of wind-tunnel wall effects for varying values of C_μ at $\alpha = -5$ deg.

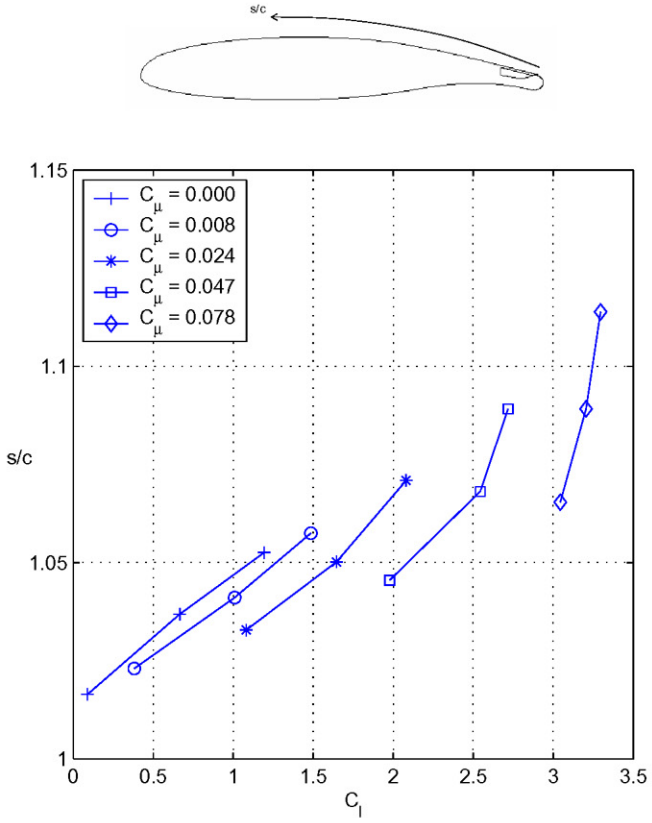

Figure 13: CC effects on stagnation-point location.

Mechanical & Aerospace Engineering

CFD Analysis of a Circulation Control Airfoil Using Fluent

Greg McGowan
M.S. Candidate
gzmcgowa@ncsu.edu

Ashok Gopalarathnam
Assistant Professor
ashok_g@ncsu.edu

NCSU Applied Aerodynamics Group
Mechanical and Aerospace Engineering
North Carolina State University, Raleigh, NC

NASA/ONR 2004 Circulation Control Workshop
Hampton, VA
16-17 March, 2004

Mechanical & Aerospace Engineering

Outline

- Background & Motivation
- Geometry
- Grid Details
- Solver Details
- Results
- Conclusions

Mechanical & Aerospace Engineering

Background & Motivation

- A recent NCSU Applied Aero Group (APA) accomplishment in adaptive aerodynamics
- NCSU APA long-term goal in CC
- Current CC project in collaboration with Dr. Greg Jones, NASA LaRC

Mechanical & Aerospace Engineering

Recent NCSU APA Accomplishment

- Aerodynamics for adaptive aircraft
- Recent successful work on auto-adaptive airfoil (TE flap)

Example:
NASA NLF(1)-0215F at Re = 6 million

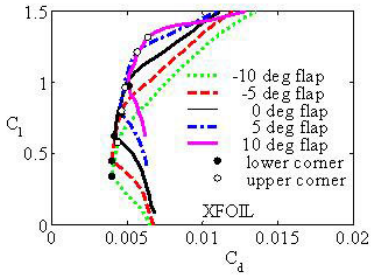

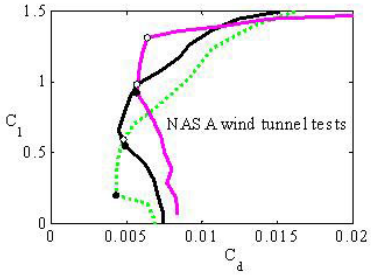

Mechanical & Aerospace Engineering

Long-term NCSU APA Goal in CC

- Adaptive jet-flap/CC concept

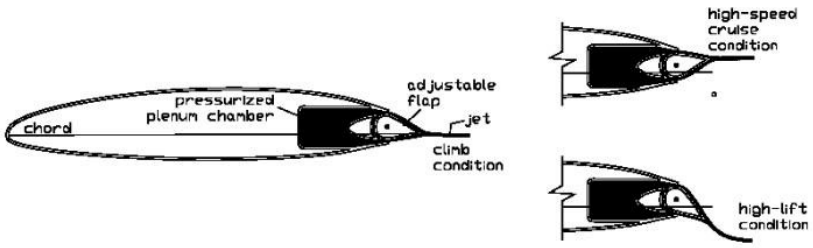

Mechanical & Aerospace Engineering

Current CC Research Project

- In collaboration with Dr. Greg Jones (LaRC)
- Use Fluent code to analyze the GACC airfoil
- Compare results with LaRC experiments and FUN2D computations
- Build CFD expertise in CC for follow-on adaptive jet flap research

Mechanical & Aerospace Engineering

Geometry

- General Aviation Circulation Control (GACC) Airfoil (Supplied by Dr. Greg Jones)
- Designed for upper and lower blowing
- Conditions for landing/take-off conditions
  - $Re_{\infty} = 533{,}000$
  - $M_{\infty} = 0.1$

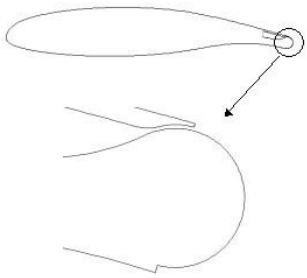

Mechanical & Aerospace Engineering

Grid Details

- Generated using Gambit
- Hybrid unstructured grid
- Structured near airfoil
- Unstructured in far-field
- ~ 20 chord lengths
- 132762 elements

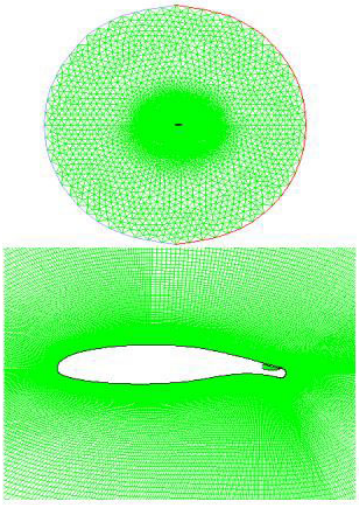

Mechanical & Aerospace Engineering

Solver Details

- Fluent version 6.1
- Steady
- Coupled-Implicit
- Node-based discretization
- Spalart-Allmaras turbulence model

Mechanical & Aerospace Engineering

Results

- Current Fluent work compared to Jones et al. (2002)
  - Experiment
  - FUN2D CFD analysis
- Parametric study of α and $C\mu$ variations

Mechanical & Aerospace Engineering

Comparison of Lift Characteristics

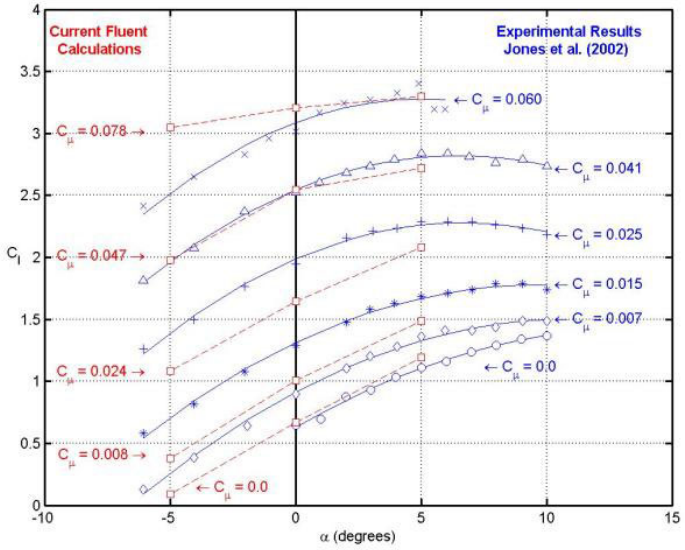

Mechanical & Aerospace Engineering

Parametric Studies

- Increasing C_μ at $\alpha = 0^o$
- Increasing α at $C_\mu = 0.047$
- Increasing α at $C_\mu = 0.078$

Mechanical & Aerospace Engineering

Increasing C_μ
$\alpha = 0°$

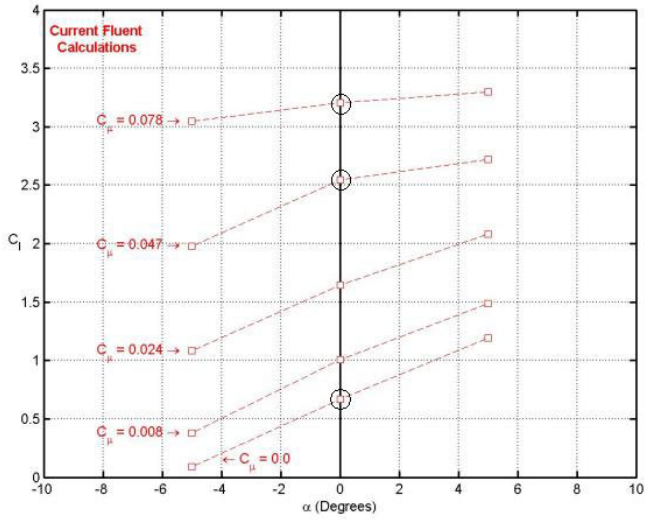

Mechanical & Aerospace Engineering

CC Effects on Streamlines
($\alpha = 0°$)

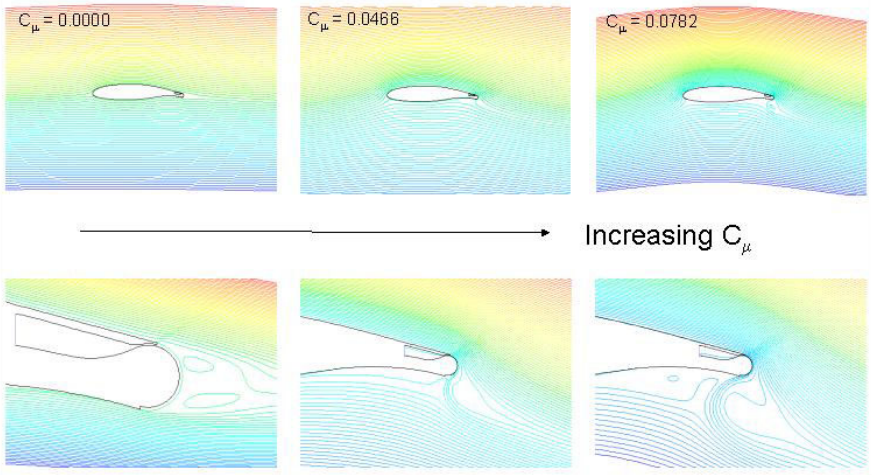

Mechanical & Aerospace Engineering

Trends in Lift and Pressure Coefficient ($\alpha = 0°$)

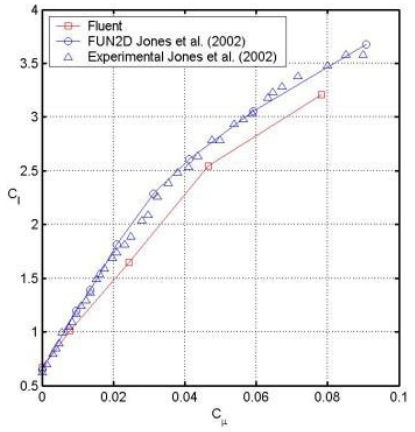

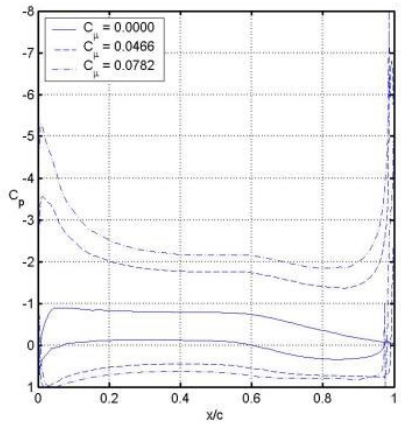

Mechanical & Aerospace Engineering

Increasing α $C_\mu = 0.047$

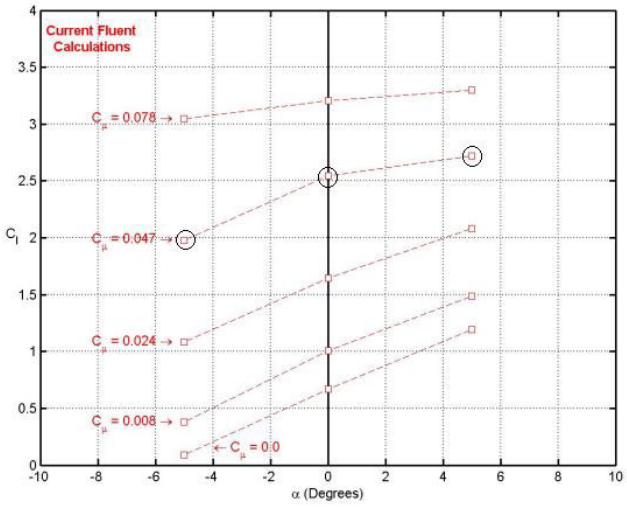

Mechanical & Aerospace Engineering

Increasing α
$C_\mu = 0.047$

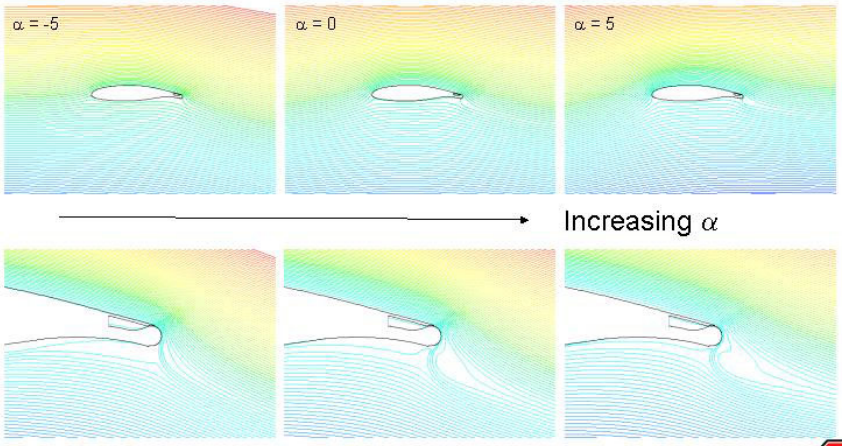

Mechanical & Aerospace Engineering

Airfoil Surface Pressure Coefficient
$C_\mu = 0.047$

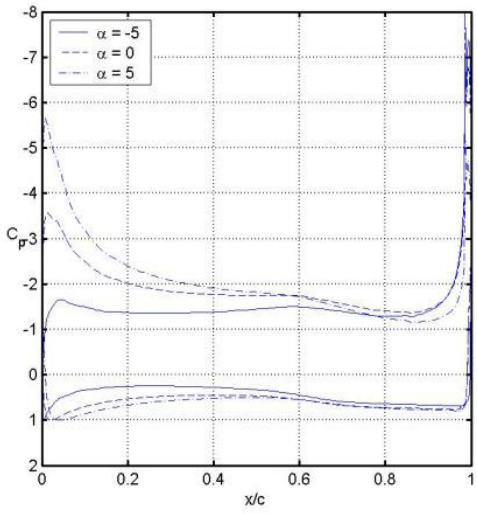

Mechanical & Aerospace Engineering

Increasing α
$C_\mu = 0.078$

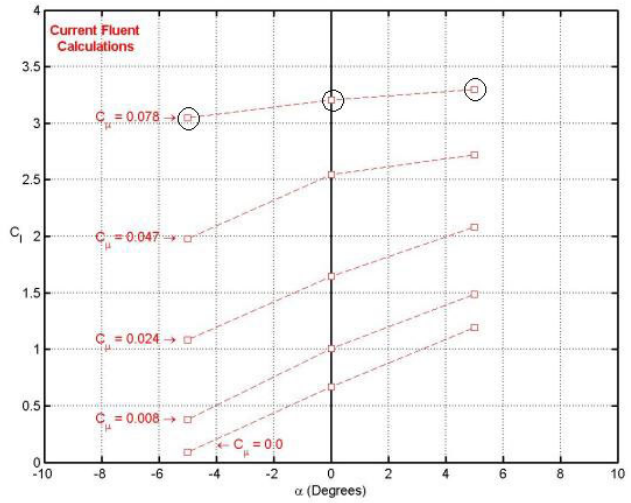

Mechanical & Aerospace Engineering

Increasing α
$C_\mu = 0.078$

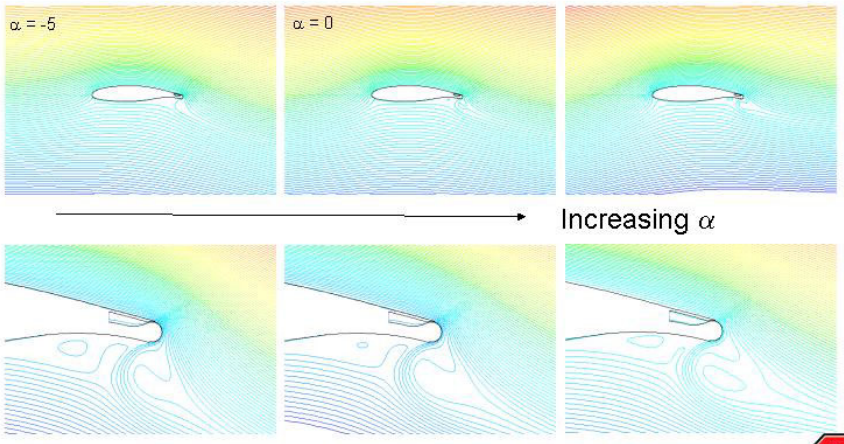

Mechanical & Aerospace Engineering

Airfoil Surface Pressure Coefficient

$C_\mu = 0.078$

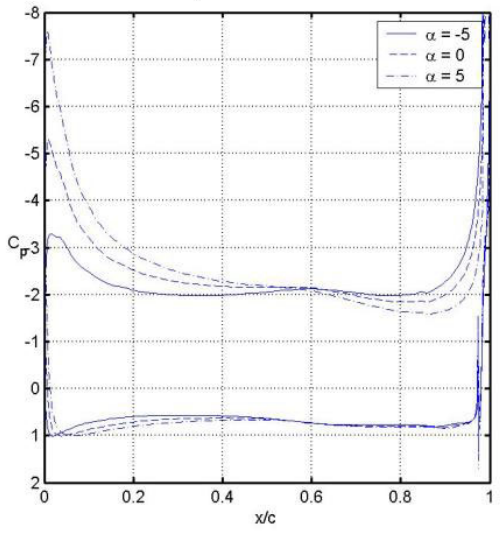

Mechanical & Aerospace Engineering

CC Effect on LE Stagnation Point

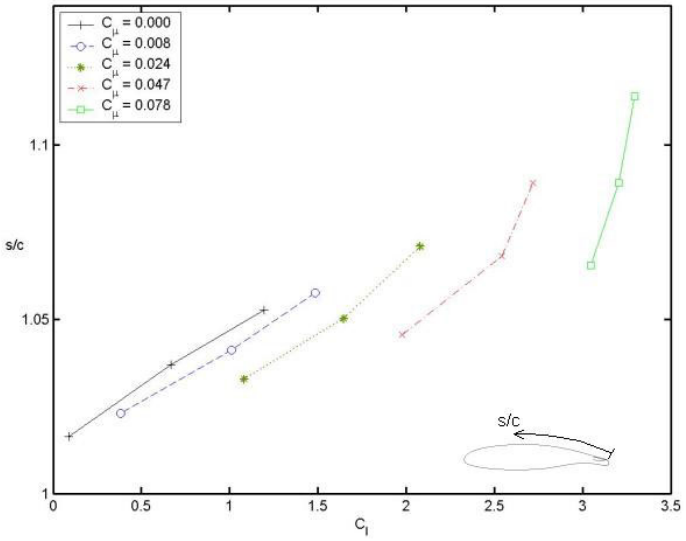

Mechanical & Aerospace Engineering

Conclusions

- CFD computations performed for GACC with Fluent
- Trends and much of data compare well with LaRC experiments and FUN2D
- Typical run time of 1.5-2.5 days per case (Pentium Xeon 3.0 GHz)
- Systematic movement of LE stagnation point can be used for sensing and closed-loop control
- Provides foundation for adaptive jet flap/CC research

Mechanical & Aerospace Engineering

Acknowledgements

- Dr. Gregory S. Jones for geometry, data, and helpful discussions

Mechanical & Aerospace Engineering

Supplemental Slides

Mechanical & Aerospace Engineering

Mach contours for increasing Cμ

$\alpha = 0$

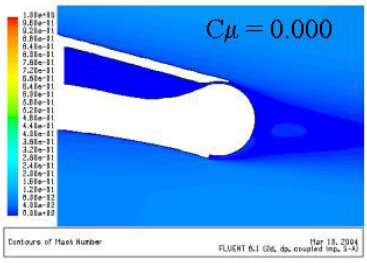

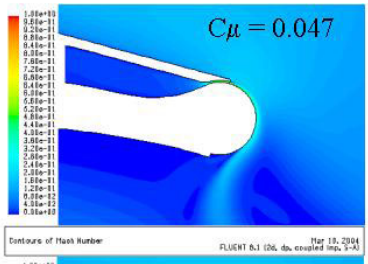

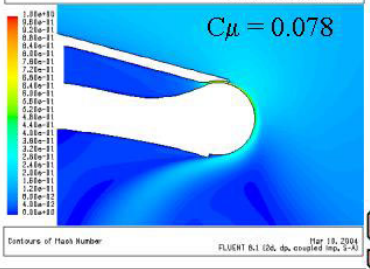

Mechanical & Aerospace Engineering

Mach contours for increasing α
$C\mu = 0.047$

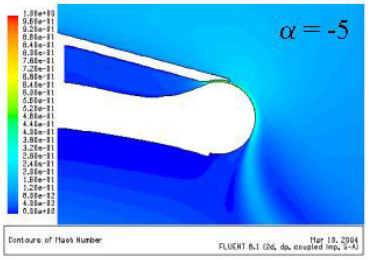

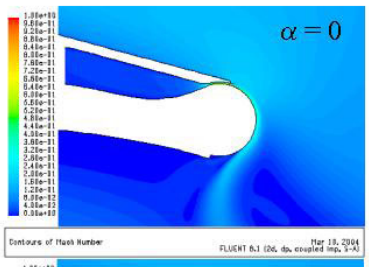

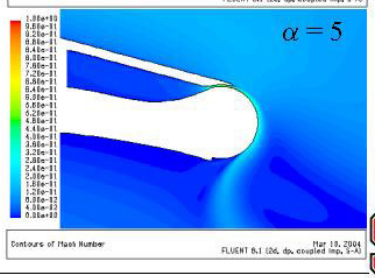

Mechanical & Aerospace Engineering

Mach contours for increasing α
$C\mu = 0.078$

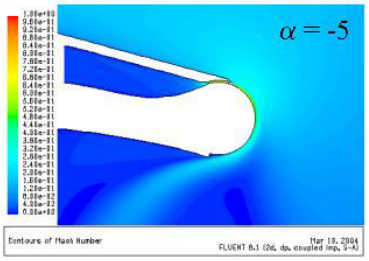

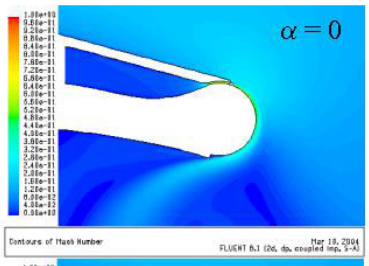

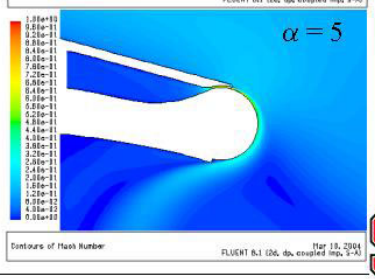

Mechanical & Aerospace Engineering

Typical Residual Plot

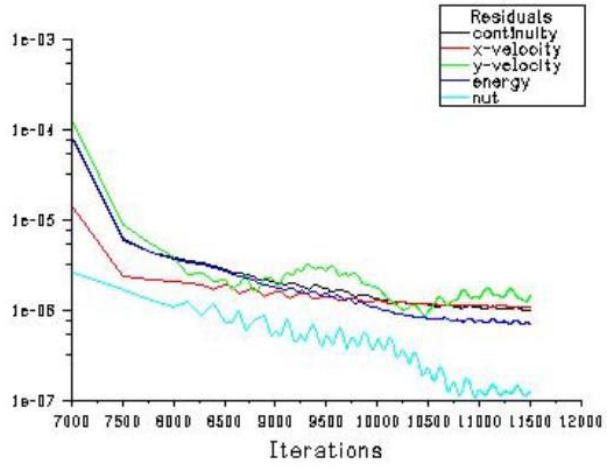

Mechanical & Aerospace Engineering

Cruise Flaps for NLF Airfoils

- Trailing-edge flaps or "cruise flaps" can be used to shift the drag bucket of an airfoil.
- Originally conceived by Pfenninger (1947)

Example:
NASA NLF(1)-0215F at Re = 6 million

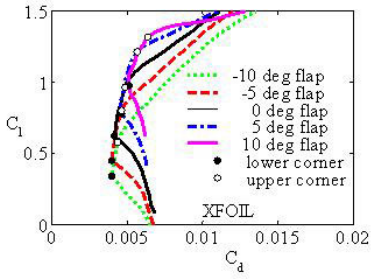

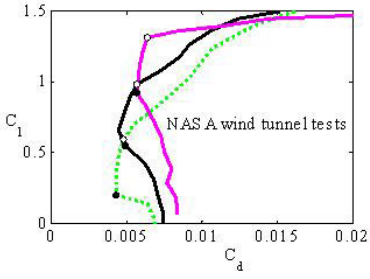

Stagnation-point Sensing

- Cruise flaps work by maintaining the stagnation point within a small desirable region near the leading edge (well known)

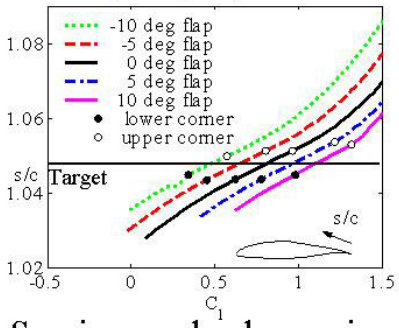

Example:
NASA NLF(1)-0215F

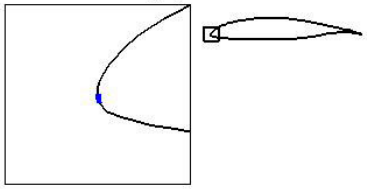

- Sensing can be done using surface hot-film array